High Temperature Creep Damage Under Biaxial Loading—Part II: Model and Simulations

F. Trivaudey

P. Delobelle

Laboratoire de Mécanique Appliquée
– URA 279 CNRS,
Faculté des Sciences et des Techniques,
25030 Besancon, Cedex, France

The inadequacies, in describing the high temperature creep damage of two industrial alloys (Part I) with a model where the anisotropic damage variable D depends only on time have been pointed out. It is therefore proposed to introduce directly strain rate in the damage law. This rule is then integrated into a unified viscoplastic model, with internal variables, that has been developed elsewhere. Some numerical simulations obtained with the complete formulation are reported and, in general, yield acceptable results.

1 Introduction

In Part I [1], the respective influence of the Von-Mises equivalent stress $\bar{\sigma}$ and of the maximum principal stress σ_{p1} on the high temperature creep damage of two industrial alloys (INCO 718 and 17 – 12 SPH stainless steel) are pointed out in a quantitative way through tensile-torsion biaxial tests. Through inversions of the shear component, the important part taken by the principal direction $\mathbf{n}_{p1}$ corresponding to the maximum principal stress has been shown. Opposite results are observed according to whether the alloy suffers cyclic hardening (17 – 12 SPH) or cyclic softening (INCO). These results are supported by metallographic observations. The effects, on the rupture time and rupture strain of a short preloading (prestrain effect) are pointed out.

In this part, the interpretation and the modeling of such behavior are presented.

2 Interpretation and Modeling

2.1 Damage Evolution Laws

(*i*) *Classical Approach.* The one-dimensional analysis of Rabotnov-Kachanov [2–4] leads to a damage variable obeying the equation:

$$\dot{D}/\dot{D}_0 = (\sigma/\sigma_0)^{\nu}(1/(1-D))^{\eta}, \tag{1}$$

where $\dot{D}_0$ and σ_0 are dimensional constants. Its solution predicts a rupture time, (for a critical damage $D^* = 1$) given by:

$$t_R = (1/(\eta+1)\dot{D}_0)\,(\sigma_0/\sigma)^{\nu}. \tag{2}$$

The generalization of (1) and (2) to the case of complex stress states can be obtained using a function $\Delta(\sigma_{ij}/\sigma_0)$ of the stress tensor invariants. In such a way, Hayhurst [5] introduces a linear functions of the maximum principal stress σ_{p1}, the first stress invariant J_1 and the second invariant of the deviatoric stress $J_2^{1/2} \propto \bar{\sigma}$. Contrary to the ductile plastic rupture case, the part of J_1 is generally negligible during creep. Analyses based on material science use a product of the previous invariants [6–8]. In the present case, as in equation (6), Part I, $\nu = \nu_1 + \nu_2$, $\Delta(\sigma_{ij}/\sigma_0)$ may be written as:

$$\Delta(\sigma_{ij}/\sigma_0) = (\sigma_{p1}^{\nu_2} \cdot \bar{\sigma}^{(\nu-\nu_2)}/\sigma_0^{\nu}))^{1/\nu}, \tag{3}$$

thus corroborating Cane's results [8]. Clearly, relationship (3) predicts $D = 0$ in a purely compressive test for which the maximum principal stress is zero; this might disagree with experiments. To verify this and assess for damaging capability of compressive states of stress, several cyclic creep tests with rectangular shaped cycles (i.e., tension, torsion with inversion, compression) including holding times in the compressive state are being performed. In addition, different tension-internal pressure test are under way in order to verify the small influence of J_1 (or J_3). Therefore, relationship (3) will be retained in the present state of the study; however, it might further appear that a contribution of a compressive state of stress to damage should be accounted for; which could be obtained through an additive combination of σ_{p1} and $\bar{\sigma}$.

Taking into account the influence of the principal direction $\mathbf{n}_{p1}$ can be obtained through the introduction of the second rank tensor $(\mathbf{n}_{p1} \otimes \mathbf{n}_{p1})$, i.e., the tensor product of $\mathbf{n}_{p1}$. Thus, the tensor $\mathbf{D}$ is defined as:

$$\left.\begin{aligned} &\dot{D}_{ij} = \dot{D} \cdot (\mathbf{n}_{p1} \otimes \mathbf{n}_{p1})_{ij}, \text{ together with:} \\ &\dot{D}/\dot{D}_0 = \left((\sigma_{p1}^{\nu_2} \cdot \bar{\sigma}^{(\nu-\nu_2)}/\sigma_0^{\nu}) \cdot (1/(1-D))^{\eta} \right), \\ &\qquad \text{with } \nu_2 = \nu(\sigma_{p1}/\sigma_R), \\ &\text{or in another contracted form:} \\ &\frac{\dot{D}}{\dot{D}_0} = \left(\left(\frac{\bar{\sigma}}{\sigma_0}\right) \left(\frac{\sigma_{p1}}{\bar{\sigma}}\right)^{\left(\frac{\sigma_{p1}}{\sigma_R}\right)} \right)^{\nu} \left(\frac{1}{1-D}\right)^{\eta}. \end{aligned}\right\} \tag{4}$$

$\nu = 9$ for the 17 – 12 SPH and $\nu = 14$ for the INCO alloy.

The equations (4) constitute a simple approach to damage in agreement with the experimental results about the rupture

Contributed by the Materials Division for publication in the JOURNAL OF ENGINEERING MATERIALS AND TECHNOLOGY. Manuscript received by the Materials Division April 18, 1989; revised manuscript received December 28, 1989.

times for monotonic loadings and which can be solved in an analytical way.

A more complete theoretical modeling was proposed by Murakami et al. [9, 10]. It consists in extending the uniaxial Rabotnov-Kachanov basic concept of an effective stress $\tilde{\sigma} = (\sigma/(1 - D))$ to the stress tensor. For this, a second rank tensor Φ is defined as:

$$\Phi = (\mathbf{I} - \mathbf{D})^{-1} \text{ (I unit tensor)}, \tag{5}$$

and the effective stress tensor, symmetrical, of the order two $\tilde{\sigma}$, is given by:

$$\tilde{\sigma} = 1/2(\sigma\Phi + \Phi\sigma). \tag{6}$$

By analogy to the processes leading to (2) and (3) one can write:

$$\dot{D}_{ij}/\dot{D}_0 = (\tilde{\sigma}_{p1}^{\nu_2} \cdot \bar{\tilde{\sigma}}^{(\nu-\nu_2)}/\sigma_0^{\nu}) \cdot \bar{\Phi}^{\eta-\nu} \cdot (\mathbf{n}_{p1} \otimes \mathbf{n}_{p1})_{ij}, \tag{7}$$

where: $\bar{\Phi} = (\Phi_{ij}\Phi_{ij})^{1/2}$, $\bar{\tilde{\sigma}} = \sqrt{\frac{3}{2}(\tilde{\sigma}'_{ij}\,\tilde{\sigma}'_{ij})^{1/2}}$, $\tilde{\sigma}'_{ij}$ being a component of the deviatoric effective stress. It must be noticed that no Φ invariant leads to $(1/(1 - D))$ when the uniaxial case is considered and the term $(\bar{\Phi}^{(\eta-\nu)})$ is retained in (7), in the same way as $\eta \neq \nu$ is introduced in (1). The inequality, $\eta \neq \nu$ has no clear physical meaning but it provides a supplementary parameter aimed at improving the fitting of the experimental creep curves by the model as does the factor $(\bar{\Phi}^{(\eta-\nu)})$. In view of the ambiguity in the meaning of this term, the analysis which follows will assume $\eta = \nu$.

It must be noticed that when the same rupture time in uniaxial tensile tests is taken for the two models, (4) and (5) to (7), their respective numerical predictions with respect to proportional tensile-torsion curves are close to each other.

The damage evolution laws (5) to (7) introduced above make damage depend only on time in creep tests, therefore t_{Ri}/t_R determination does not depend on the flow rules. t_{Ri}/t_R was calculated with $\eta = \nu$ in equations (5) to (7). The two extreme cases for INCO: $\nu = \nu_2$ or $\nu_2 = 0$ are reported in Fig. 4. In the completely anisotropic case (first one, curve 2 in Fig. 4), t_{Ri}/t_R increases from 1 to 2 when $\Delta\psi$ is changed from 0 to 90 deg. On the contrary, use of the average experimental values for ν and ν_2, leads to a predicted ratio t_{Ri}/t_R always smaller than 2 (curve 1 in Fig. 4). Moreover, Fig. 4 also shows that damage anisotropy is larger for the stainless steel 17 - 12 SPH than in the INCO alloy, which agrees with experiments.

However the model predicts that t_{Ri}/t_R can never exceed two or be less than one and is not in agreement with the experiments. In addition, this formulation predicts the rupture time to be independent of pre-hardening effects, which is in contradiction to the results reported in paragraph 3.6, Part I.

Actually, as previously mentioned, it is likely that damage does not depend only on time but also on strain or strain rate; therefore damage rules and flow rules can no longer be separated. This remark agrees with the conclusion drawn from the work of Hales [11] and Majumdar et al. [12] relative to the study of the creep-fatigue interaction phenomena in a 304 and 316 type steels in the neighborhood of 600°C. Adding a strain parameter aimed at accounting for the cyclic properties of the material should give more freedom on the predicted evolution of t_{Ri}/t_R and make it possible to get $t_{Ri}/t_R \leq 1$ for cyclic softening and $t_{Ri}/t_R \geq 2$ for materials exhibiting cyclic hardening. The analysis of such a model is presented in the next paragraph. It is worth noting at this point that, contrary to present equations (4) to (7), Pineau et al. proposed a model in which only strain is taking a part [13, 14].

(*ii*) *New Approach.* The hypothesis that the tensor product takes into account the damage anisotropy is not challenged. In fact, microscopic observations have clearly shown the role of σ_{p1} and of its associated principal direction. An attempt could be made to modify the scalar component which expresses the amplitude of the damage, and a simple way to introduce the strain into the damage kinetics is to write:

$$\frac{\dot{D}}{\dot{D}_0} = \Delta^{\nu}\left(\frac{\tilde{\sigma}_{ij}}{\sigma_0}\right)\left(\gamma + (1-\gamma)\left(\frac{\bar{\dot{\epsilon}}}{\bar{\dot{\epsilon}}_1}\right)^{\rho}\right) \text{ with}$$

$$\bar{\dot{\epsilon}} = \left(\frac{2}{3}\,\dot{\epsilon}_{ij}\dot{\epsilon}_{ij}\right)^{1/2}, \tag{8}$$

where $\bar{\dot{\epsilon}}_1$ represents a normalization strain rate and coincides with the minimum (or steady) strain rate corresponding to the imposed stress state. γ is a parameter allowing to weighting of the relative effects of time and strain. ρ is a supplementary parameter that is taken equal to unity. $\Delta^{\nu}(\tilde{\sigma}_{ij}/\sigma_0)$ results from equation (7), and the minimum strain rate can be written, in accordance with experimental observations, in the form:

$$\bar{\dot{\epsilon}}_1 = A\bar{\sigma}^m\sigma_{p1}^n, \text{ with } m + n = \nu. \tag{9}$$

It can be noted that with $\rho = 1$ and for a uniaxial loading, equation (8) has analytical solutions in the two extreme cases where $\gamma = 0$ and $\gamma = 1$, which allows the determination of the ratio $(\dot{D}_0/\sigma_0^{\nu})$ for a fixed critical damage D^*.

However, two distinctions should be made relative to the formulation (8). First of all, considering the behavior of each material during tests with inversion of the torsion component, it can be assumed that no damage occurs due to the strain during the hardening phase. More generally, each time that the equivalent strain rate decreases, it is assumed that there is no damage connected with the strain and only the damage connected with time remains. On the other hand, as soon as the strain rate increase, this growth being a function of time, then a damage term is introduced due to the strain. This comes down to testing the sign of the derivative of $\bar{\dot{\epsilon}}$. It can be noted that in this formulation, it is time that causes $\bar{\dot{\epsilon}} > 0$ and thus starts the strain damage. Secondly, the developed damage law is integrated into a unified viscoplastic model [15, 16], that is to say, only one type of strain is considered and the large strains connected with the loading contribute in the same way as the smaller viscoplastic strains to the evolution of strain damage. The hypothetical damage created during the loading path is essentially ductile and does not appear until a critical strain ϵ_c is reached [3, 4]. This case is treated by another formulation [3, 4]. It is for this reason that a criteria is introduced which allows the loading phase to be recognized. Thus, when there is a variation of applied stress, the part of the damage connected with the strain must be set equal to zero. It can be noted that with the partitioned model [17], this separation is realized directly since plastic and viscous strains are dissociated. To summarize, considering the distinctions that have been made and equations (5) to (9), the damage laws can be written:

$$\left.\begin{aligned}
&\frac{\dot{D}_{ij}}{\dot{D}_0} = \Delta^{\nu}\left(\frac{\tilde{\sigma}_{ij}}{\sigma_0}\right) \cdot \left[\gamma + (1-\gamma)\,\frac{\bar{\dot{\epsilon}}}{\bar{\dot{\epsilon}}_1}\,H(\bar{\dot{\epsilon}})(1 - H(\bar{\tilde{\sigma}}))\right](\mathbf{n}_{p1} \otimes \mathbf{n}_{p1})_{ij},\\
&\text{where } H(\,.\,) \text{ is the Heaviside function:}\\
&\quad H(x) = 1 \text{ if } x > 0 \text{ and } H(x) = 0 \text{ if } x \leq 0\\
&\quad \Phi = (\mathbf{I} - \mathbf{D})^{-1}, \tilde{\sigma} = 1/2\,(\sigma\Phi + \Phi\sigma) \text{ and}\\
&\quad \Delta^{\nu}\left(\frac{\tilde{\sigma}_{ij}}{\sigma_0}\right) = \frac{\tilde{\sigma}_{p1}^{\nu_2}\,\bar{\tilde{\sigma}}^{(\nu-\nu_2)}}{\sigma_0^{\nu}} \text{ with}\\
&\quad \bar{\dot{\epsilon}}_1 = A\bar{\sigma}^m\sigma_{p1}^n \text{ and } \nu_2 = \nu(\sigma_{p1}/\sigma_R).
\end{aligned}\right\} \tag{10}$$

2.2 Flow Rules. It has already been mentioned that cyclic properties and the flow direction rotations (Fig. 7, Part I) are

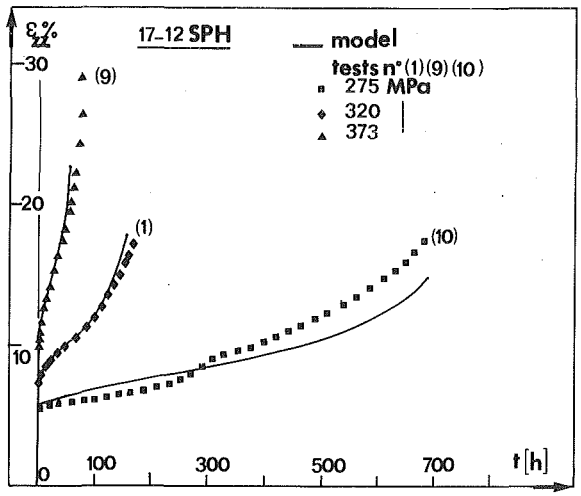

Fig. 1 Examples of predictions obtained on the 17 - 12 SPH Steel from equations (10) and (12) to (27). Uniaxial case with different stress levels.

accounted for through two internal variables (Y and α), respectively, isotropic and kinematic, the recovery of which is not negligible because of the high temperatures. A unified model developed by the authors [15, 16] and identified for undamaged states of the two considered alloys gave very satisfactory predictions.

At this stage of the modelization it remains to couple the damage law (10) to the behavior laws, that is to say, to explicit the effect of damage on the behavior of the material. Considering the form of equation (6) for the effective stress $\tilde{\sigma}$, in agreement with Murakami et al. [10, 18], the effective stress tensor $\tilde{\mathbf{S}}$, which takes part in the behavior laws, can be defined in two ways:

—either in an anisotropic fashion by the intermediary of a fourth order tensor $\underline{\underline{\gamma}}(\Phi)$ relating $\tilde{\mathbf{S}}$ to σ:

$$\tilde{\mathbf{S}} = 1/2(\underline{\underline{\gamma}}(\Phi)\sigma + (\underline{\underline{\gamma}}(\Phi)\sigma)^T), \tag{11}$$

—or in an isotropic fashion by the intermediary of an invariant of $\mathbf{D}$, for example the first:

$$\tilde{\mathbf{S}} = (1 + c \text{ trace } \mathbf{D})\sigma. \tag{12}$$

In order to avoid unnecessary complexity and in view of the fact that the density of defects remains small even at rupture, the second solution will be adopted. In addition, it can be noted that the parameter c plays a direct role in the behavior law and thus offers the supplementary possibility of adjusting the rupture strain as a function of the loading conditions. Taking into account the experimental observations that show that the rupture strain strongly depends on σ_{p1}, (Figs. 1(a) and 1(b)), it can be written:

$$c = (1 + c_0)\frac{\sigma_{p1}}{\sigma} - c_0, \tag{13}$$

where c_0 is a constant.

Equations (12) and (13) constitute the mode in which the damage will influence the behavior laws.

Without entering into the mathematical details of the model explicited in references [15] and [16], a summary of its structure and a complete formulation with the introduction of damage will be given.

(i) *The Unified State Equation.* The model in question is a unified model, which is to say, that only one type of strain is considered and it is of a viscoplastic nature; the time independent plasticity is an asymptotic condition of the present formulation (exponential branch of equation (14)). This model is essentially of a kinematic and viscous character (introduction of the kinematic tensor variable α_{ij}). The scalar variable Y is used, on one hand, to define a yield surface F allowing the distinction between a state of loading or unloading in the space of internal variables, and on the other hand, to control the evolution of the viscous component with the strain.

$$\frac{\dot{\epsilon}_{ij}}{\dot{\epsilon}_0} = \frac{3}{2}\left(\frac{K(\tilde{Y})}{\sigma_0^*}\right)^{n*} \cdot \left(\sinh\left(\frac{\overline{\tilde{S}-\tilde{\alpha}}}{K(\tilde{Y})}\right)^{n*}\right)\frac{\tilde{S}'_{ij} - \tilde{\alpha}'_{ij}}{\overline{\tilde{S}-\tilde{\alpha}}}, \tag{14}$$

where $\tilde{Y}$ and $\tilde{\alpha}$ represent the damaged internal variables, respectively, isotropic and kinematic, $\tilde{S}'_{ij}$ and $\tilde{\alpha}'_{ij}$ the damaged components of the deviatorics of $\tilde{\mathbf{S}}$ and $\tilde{\alpha}$, and $\overline{\tilde{S} - \tilde{\alpha}} = (3/2\,(\tilde{S}'_{ij} - \tilde{\alpha}'_{ij})\,(\tilde{S}'_{ij} - \tilde{\alpha}'_{ij}))^{1/2}$ the second invariant of the tensor $\tilde{\mathbf{S}} - \tilde{\alpha}$. $\dot{\epsilon}_0$, σ_0^* and n^* are the constants for a given isotherm. It is recalled that the definition of $\tilde{\mathbf{S}}$ is given by equation (12), while $\tilde{\alpha}$ and $\tilde{Y}$ are defined below (equations (17) and (19)). The increase of the viscous component σ_v with strain is assured by the function $K(\tilde{Y})$;

$$\sigma_v = K(\tilde{Y})\sinh^{-1}\left[\frac{2}{3}\frac{\bar{\dot{\epsilon}}}{\dot{\epsilon}_0}\left(\frac{\sigma_0^*}{K(\tilde{Y})}\right)^{n*}\right]^{1/n*} \text{ where}$$

$$K(\tilde{Y}) = K_0\tilde{Y} \text{ and } \bar{\dot{\epsilon}} = \left(\frac{2}{3}(\dot{\epsilon}_{ij}\dot{\epsilon}_{ij})\right)^{1/2}. \tag{15}$$

(ii) As in classical plasticity, but in the space of the internal variables, the surface F translates kinematically (introduction of the tensor variable α_{2ij}) and grows isotropically (scalar variable Y). The hypersphere F is thus written: $F = \overline{\alpha - \alpha_2} - Y = 0$. If the variable α is located on the surface $F(F = 0)$ then an active loading yielding macrostrains is defined and inversely, if α is in the interior ($F < 0$), then a passive loading yielding microstrains is defined. A transition criteria between these two states is also necessary. For a damaged material, these two kinds of strain are mathematically defined by equation (16) to (21):

—macrostrains:

$$\tilde{\alpha}_{ij} = \tilde{\alpha}_{1ij} \text{ if } \left.\begin{matrix}\tilde{F} = \overline{\tilde{\alpha}_1 - \tilde{\alpha}_2} - \tilde{Y} = 0 \\ \tilde{\alpha}_{1ij}\dot{\tilde{\alpha}}_{1ij} \geq 0\end{matrix}\right\}, \tag{16}$$

where $\tilde{\alpha}_2$ and $\tilde{Y}$ are defined by:

$$\left.\begin{matrix}\tilde{\alpha}_{2ij} = (1 + c \text{ trace } \mathbf{D})\,\alpha_{2ij} \\ \tilde{Y} = Y/(1 + c \text{ trace } \mathbf{D})\end{matrix}\right\}, \tag{17}$$

with:

$$\left.\begin{matrix}\dot{\alpha}_{2ij} = f(\ldots.) \\ \dot{Y} = g(\ldots.)\end{matrix}\right\} \text{ (equations given below).} \tag{18}$$

In addition, there is the consistency equation ($F = \dot{F} = 0$), which prevents α_{1ij} from leaving the surface F during the macroplastic strain:

$$\dot{\tilde{\alpha}}_{1ij} = \dot{\tilde{\alpha}}_{2ij} + \dot{\tilde{Y}}/\tilde{Y}(\tilde{\alpha}_{1ij} - \tilde{\alpha}_{2ij}). \tag{19}$$

Equations (17) and (19) allow the introduction of damage into the expression for the surface F and a transition criteria. The introduction of damage in the kinematical variables α_2 is performed in the same way but only with respect to the stress (equation (12)), that is to say, isotropically by the intermediary of the factor (1 + c trace $\mathbf{D}$). The same for the variable Y, but this factor intervenes in the denominator, which leads to a diminution of Y with the damage since experimentally the elastic limit, for a given offset, decreases with damage. The definition of α is performed directly by the consistency equation (19) associated with the derivatives of equations (17):

—microstrains:

$$\tilde{\alpha}_{ij} = \tilde{\alpha}_{1ij} \text{ if } \left.\begin{matrix}\tilde{F} = \overline{\tilde{\alpha}_1 - \tilde{\alpha}_2} - \tilde{Y} < 0 \\ \text{or} \\ \tilde{F} = 0 \text{ and } \tilde{\alpha}_{1ij}\dot{\tilde{\alpha}}_{1ij} < 0\end{matrix}\right\}, \tag{20}$$

Table 1 Material constants for the two considered alloys: 17 - 12 SPH and INCO

- **Damage parameters**

	17-12 SPH	INCO 718
ν	8	12
$\eta=\nu$	-	-
ν_2	σ_{p1}/σ_R with σ_R = 580 MPa	1.2
γ	0.12	0.5
ρ	1	1
m	7.6	13.5
n } m+n=ν	0.4	-1.5
A	$9.18\ 10^{-28}\ s^{-1}(MPa)^{-8}$	$9.5\ 10^{-43}\ s^{-1}(MPa)^{-12}$
D^*	0.3	0.2
c_0	0.6	-1(C=1)
$(\dot{D}_0/\sigma_0^{\nu})$	$1.13\ 10^{-27}\ s^{-1}(MPa)^{-8}$	$1.15\ 10^{-41}\ s^{-1}(MPa)^{-12}$

- **Flow rule parameters**

	17-12 SPH	INCO 718
$\dot{\epsilon}_0$	$1.7\ 10^{-12}\ s^{-1}$	$3\ 10^{-33}\ s^{-1}$
σ_0^*	0.15 MPa	1 MPa
n^*	2.2	12
K_0	0.13	-
P_2	450	427
R_2	$9.34\ 10^{-34}\ s^{-1}(Nm^{-2})^{-8}$	$5.5\ 10^{-25}\ s^{-1}(Nm^{-2})^{-2}$
I_0	3.5	2
b	10	200
R_1	$5.8\ 10^{-28}\ s^{-1}(Nm^{-2})^{-8}$	-
Y_0	65 MPa	730 MPa
b^{sat}	$3.5\ 10^3$	-
Y_{∞}^{sat}	230 MPa	$Y^{sat}-Y_{\infty}^{sat}$=650 MPa
Y_0^{sat}	65 MPa	-
η^*	0.04	-
P_1	$4.4\ 10^5$	$4.7\ 10^3$
r_m	$1.63\ 10^{-4}\ s^{-1}$	-
β	$4.5\ 10^{-9}(Nm^{-2})^{-1}$	-
M_0	8	-

and in this case, the kinematic equations are given by:

$$\left.\begin{aligned}\dot{\alpha}_{1ij}&=h(\ldots.),\}\\ \dot{\alpha}_{2ij}&=f(\ldots.)\\ \dot{Y}&h(\ldots.).\end{aligned}\right\} \quad (21)\ (18)$$

The group of equations (18) and (21) is given below in (iii).

(iii) The Kinetic Equations for α_2, Y and α_1. These equations govern the evolution of the surface $\tilde{F}$ and thus those of α via the consistency equation in the case of macrostrains (equations (19) and (22)) and directly in the case of microstrains. These equations are constructed following the classical approach of Bailey-orowan where hardening and recovery are two antagonistic phenomena. It can be remarked that the hardening terms are nonlinear and that a recovery term is present, made necessary on account of the stress domain and the elevated temperatures. The damage plays an explicit role only in recovery terms, as the hardening terms are already affected by the intermediary of the strain-rate.

$$\left.\begin{aligned}\dot{\alpha}_{2ij}&=p_2\left(\frac{2}{3}\,Y\dot{\epsilon}_{ij}-\alpha_{2ij}\dot{\bar{\epsilon}}\right)-R_2(Y-\tilde{\alpha}_2)(\overline{\tilde{\alpha}_2-\tilde{\alpha}_{02}})^{L0}\,\frac{\tilde{\alpha}_{2ij}-\tilde{\alpha}_{02ij}}{\tilde{\alpha}_2-\tilde{\alpha}_{02}}\\ \dot{Y}&=b(Y^{sat}-Y)(\dot{\bar{\epsilon}}-R_1|Y-Y_{01}|^{L0}\,\mathrm{sign}\,(Y-Y_{01}))\end{aligned}\right\}, \quad (22a,b)$$

with the initial conditions: $\alpha_{2ij}(0) = 0$ and $Y(0) = Y_0 < Y^{sat}$ for cyclic hardening, $Y_0 > Y^{sat}$ for cyclic softening. $\tilde{\alpha}_2 = \{3/2\ (\alpha'_{2ij}\ \alpha'_{2ij})\}^{1/2}$ and $\overline{\tilde{\alpha}_2-\tilde{\alpha}_{02}} = (3/2\ (\tilde{\alpha}'_{2ij}-\tilde{\alpha}'_{02ij})\ (\tilde{\alpha}'_{2ij}-\tilde{\alpha}'_{02ij}))^{1/2}$. L_0, R_1, R_2, p_2, and b are constants, $\tilde{\alpha}_{02}$ and Y_{01} are the maximum nonrecoverable values of α_2 and Y, whose expressions have been given in detail in references [15-16].

In order to take into account the cyclic properties and in particular, the effects of partial memorization of the prestrains, Y^{sat} (equation (22*b*)) is related to a memory variable q, such that:

$$\dot{Y}^{sat}=b^{sat}(Y_{\infty}^{sat}-Y^{sat})\dot{q}\ \text{with}\ Y_{(0)}^{sat}=Y_0^{sat}, \quad (23)$$

b^{sat} and Y_{∞}^{sat} are two constants.

In agreement with Chaboche et al. [19] and Ohno [20], q is related to the evolution of a nonhardening surface G, expressed in the strain space:

$$G=(\overline{\epsilon-\zeta})-q\ \text{with}\ \overline{\epsilon-\zeta}=(2/3(\epsilon_{ij}-\zeta_{ij})(\epsilon_{ij}-\zeta_{ij}))^{1/2}. \quad (24)$$

ζ_{ij} represents the translation of this surface and q its maximum radius. This surface can evolute only if the strain ϵ_{ij} is located on its boundary, which implies a consistency equation of the form $G = \dot{G} = 0$. $\dot{q}$ can be written in the form:

$$\dot{q}=\eta^*H(G)<n_{ij}n_{ij}^*>\dot{\bar{\epsilon}}, \quad (25)$$

with: $n_{ij}=\sqrt{\frac{3}{2}}\,\frac{\tilde{S}'_{ij}-\tilde{\alpha}'_{ij}}{\overline{\tilde{S}-\tilde{\alpha}}}$, $n_{ij}^*=\sqrt{\frac{2}{3}}\,\frac{\epsilon_{ij}-\zeta_{ij}}{\overline{\epsilon-\zeta}}$, $H(\,.\,)$ is the previously defined Heaviside function and $\langle\ .\ \rangle$ the Macawley brackets ($\langle x\rangle = x$ if $x \geq 0$ and $\langle x\rangle = 0$ if $x < 0$). The consistency equation $G = \dot{G} = 0$ allows ζ_{ij} to be obtained as follows:

$$\dot{\zeta}_{ij}=\sqrt{\frac{3}{2}}\,((1-\eta^*)H(G)\langle n_{ij}n_{ij}^*\rangle n_{ij}^*\dot{\bar{\epsilon}}). \quad (26)$$

The parameter η^* fixes the rapidity of the establishment of the memory variable q.

The evolutionary law for $\tilde{\alpha}_{1ij}$ in the case of microstrains is given by:

$$\left.\begin{aligned}&\tilde{\alpha}_{1ij}=(1+c\ \text{trace}\ \mathbf{D})\alpha_{1ij}\ \text{and}\\ &\dot{\alpha}_{1ij}=p_1\left(\frac{2}{3}\,Y\,\dot{\epsilon}_{ij}-(\alpha_{1ij}-\alpha_{2ij})\dot{\bar{\epsilon}}\right)-r_m(\sinh\beta\ \tilde{\alpha}_1)^{M0}\,\frac{\tilde{\alpha}_{1ij}}{\tilde{\alpha}}\end{aligned}\right\}, \quad (27)$$

with $\alpha_{1ij}(0) = 0$. p_1, r_m, β and M_0 are constants and $\tilde{\alpha}_1 = (3/2\ \tilde{\alpha}'_{1ij}\ \tilde{\alpha}'_{1ij})^{1/2}$. The procedure for the introduction of damage in α_1 is identical to that used for α_2.

The complete model, identified under cyclic and monotonic loading conditions, with the damage law, is composed of equations (10) and (12) to (27).

3 Numerical Simulations

3.1 Case of 17 - 12 SPH Stainless Steel. The set of model parameters for this steel is given in Table 1. Note that the prestrains connected with the machining of the samples have been accounted for in the numerical simulations.

Note that, with the exception of the parameter γ and C_0 which remain free and thus numerically adjustable from certain experimental curves, the remaining parameters of equations (10), (12), and (13) are directly accessible from the experimental results reported in Part I. ν, ν_2 and σ_R are obtained with the aid of Figs. 3(*a*, *b*) and 12, respectively. The critical damage D^* has been determined with the aid of the metallographic study described in 3.7b. The parameters A, m, and n are directly accessible from the study of the evolution of the minimum creep rate $\dot{\bar{\epsilon}}_{min}$ with σ_{zz}, $\bar{\sigma}$ and σ_{p1} (paragraph 3.1). For a uniaxial loading and a knowledge of these parameters, it is possible to integrate analytically equation (10) in the two ex-

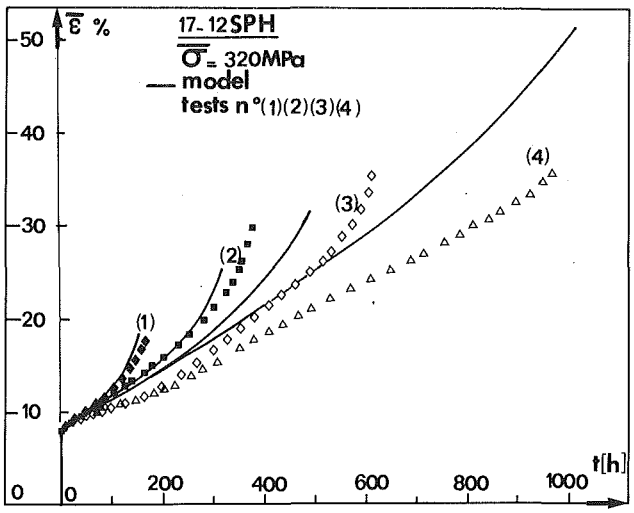

Fig. 2 Idem Fig. 1—biaxial case, influence of σ_{p1}

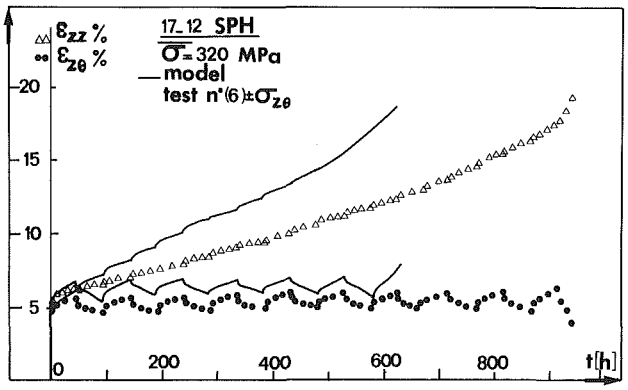

Fig. 3 Idem Fig. 1—biaxial case, effect of shear component inversion

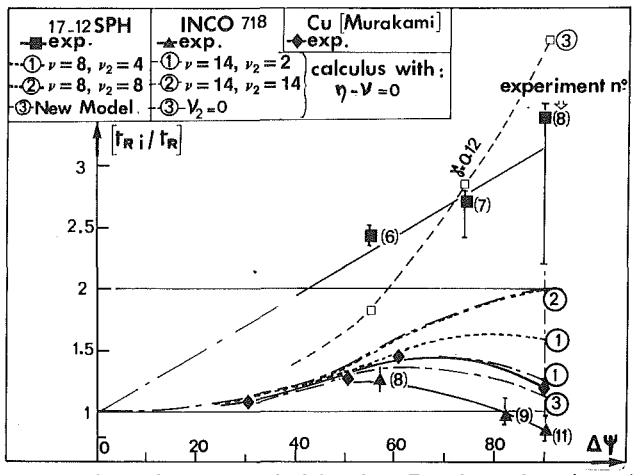

Fig. 4 Relationship between (t_{Ri}/t_R) and $\Delta\psi$. Experimental results and: — predictions obtained from equations (5) to (7) with $\nu = 8$, $\nu_2 = 4$ and $\nu = \nu_2 = 8$ in the case of the 17 - 12 SPH alloy, $\nu_2 = 2$, $\nu = 14$, $\nu = \nu_2 = 14$ and $\nu_2 = 0$, $\nu = 14$ in the case of the INCO alloy, — predictions obtained with the new model, equations (10) and (12) to (27) with $\gamma = 0.12$.

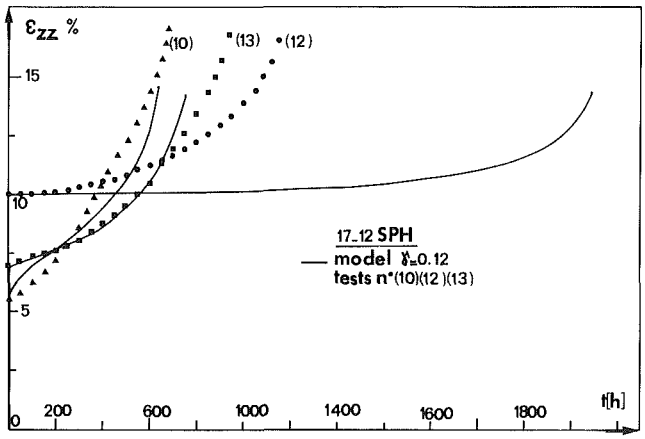

Fig. 5 Idem Fig. 1—uniaxial case, influence of the prestrain

treme cases $\gamma = 0$ and $\gamma = 1$. This allows the two values of (D_0/σ_0^r) to be determined: $(D_0/\sigma_0^r)_{\gamma=0}$ and $(D_0/\sigma_0^r)_{\gamma=1}$. In the case of the model ($\gamma \neq 0$ and 1), (D_0/σ_0^r) is calculated with the aid of the formula: $(D_0/\sigma_0^r) = \gamma(D_0/\sigma_0^r)_{\gamma=1} + (1 - \gamma)(D_0/\sigma_0^r)_{\gamma=0}$. The parameter C_0 essentially affects the strain at rupture and γ allows the damage components to be weighted by time and the strain. These two parameters are free and adjusted numerically by successive tests in such a way as to obtain a good compromise in the restitution of the experimental results reported in Figs. 1 to 5. In summary, C_0 is adjusted from the analysis of the evolution of the strain at rupture with $\bar{\sigma}$ and σ_{p1} (Fig. 2) and γ from the evolution of the ratio (t_{Ri}/t_R) (Fig. 4). The complete identification of the behavior model is out of the scope of this article, but the methodology can be found in the reference [21]. All the parameters can be experimentally determined with the aid of the following tests: tensile (Y_0), creep ($\dot{\epsilon}_0$, σ_0^*, n^*, M_0), inverse relaxation (K_0), aging under zero stress (R_2, R_1, L_0), creep hesitation measurement following stress decrements (p_1, r_m, β), and finally cyclic tests under different levels of imposed strain ($\pm \Delta\epsilon^T/2$). The establishment rate of the stabilized cycle allows the adjustment of (b, b^{sat}, Y_0^{sat} and η^*), the stress level of the stabilized cycle (Y_∞^{sat}, η^*) and the form of the stabilized cycle (P_2).

The simulated uniaxial responses are reported in Fig. 1, for different stress levels. The loading strains, the shapes of the creep curves, the time and the strain at rupture are all correctly represented. Figure 2 shows the precision with which the model reconstructs the influence of σ_{p1} on the rupture time and strain. The general agreement is acceptable. Figures 3 and 4 present the possibilities of the model with respect to the effects of shear component inversions. In contrast with the classical formulations, the ratio (t_{Ri}/t_R) can be greater than two (Fig. 4).

Finally, Fig. 5 shows the predictions, with respect to prehardening effects, notably the increase in rupture time and the quasi-insensitivity of the rupture strain.

Globally, the effects are taken into account even though the rupture times are overestimated for the larger prehardening ratios. This disagreement is certainly due to neglecting the ductile damage associated with prehardening and is apparent after a critical strain ϵ_c is reached, which was certainly the case for the larger ratios of prestrain.

In summary, the different experimental observations for this steel have, in general, been well represented by this model.

3.2 Case of INCO 718. As for the INCO 718, the situation is more difficult, both in terms of the physical damage mechanisms (the ductile damage component seems dominant) and in terms of the identification of the model (too few monotonic and cyclic tests are available in order to identify the set of model parameters). Lacking precise experimental information on the amplitude of the viscous component, there remains a large latitude for adjusting the parameters of the state equation (14), that we take in the simplified form (small argument in the sinh function (equation (14))):

$$\frac{\dot{\epsilon}_{ij}}{\dot{\epsilon}_0} = \frac{3}{2}\left(\frac{\overline{\tilde{S}-\tilde{\alpha}}}{\sigma_0^*}\right)^{n^*} \frac{\tilde{S}'_{ij} - \tilde{\alpha}'_{ij}}{\overline{\tilde{S}-\tilde{\alpha}}}. \tag{28}$$

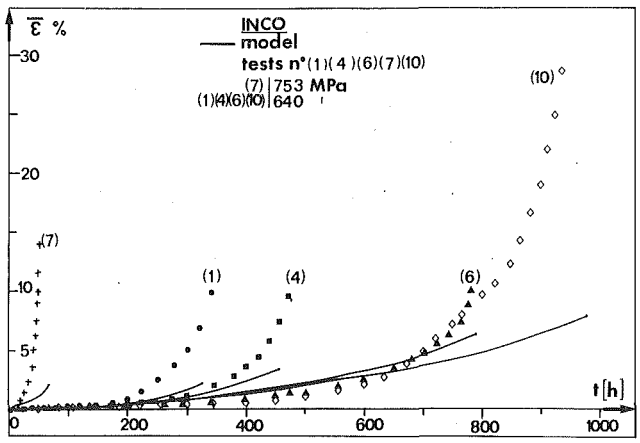

Fig. 6 Examples of predictions obtained on the INCO alloy from equations (10), (12), (13), (28) and (16) to (27). Note that the rupture strains are underestimated.

Figure 6 shows the first simulations obtained with the aid of a complete model whose parameters are reported in Table 1. The identification method for the damage parameters is identical to that mentioned for 17 - 12 SPH. Note that the rupture times are correctly described but that the rupture strains are strongly underestimated. As mentioned earlier, this disagreement is certainly connected to the neglect of the ductile damage which lead to too weak nonlinearity for the damage variable. This agrees with the analysis of Saanouni [22] who showed that the rupture strains can be correctly described, for these tests, by introducing a strongly nonlinear function of D into the state equation (14), which amounts to strongly increasing the viscous component. This lead, in the first approximation, to replace equation (12) by:

$$\tilde{\mathbf{S}} = \frac{1}{K(D)}(1 + c \text{ trace } \mathbf{D})\,\sigma \text{ with } K(D)$$

$$= K_s + (K_0 - K_s)\exp - \omega D, \tag{29}$$

where D is the scalar part of the damage (equation (8) or (10)), K_s, K_0, and ω are constants, with the condition $K_0 > K_s$.

4 Conclusions

The part taken in damage by the equivalent stress $\tilde{\sigma}$, the maximum principal stress σ_{p1} and the corresponding principal direction $\mathbf{n}_{p1}$ has been pointed out through torsion-tensile creep experiments and this on two alloys having different mechanical behaviors. Damage rules using a damage tensorial variable in a way close to the model of Murakami et al. [9, 10] are proposed; they are aimed at completing a model including kinematical and isotropic hardening variables. The inadequacies of a model where $\mathbf{D}$ depends only on time, (Rabotnov — Kachanov extensions) i.e., the failure to predict the evolution of the t_{Ri}/t_R ratio ($t_{Ri}/t_R \geq 2$ and/or ≤ 1), the underestimation of rupture strains and the failure to predict the effects of preloading the samples are pointed out.

In order, to improve upon this model, a damage formulation is proposed in which the strain directly intervenes. It is then integrated into a unified viscoplastic model developed elsewhere. Some numerical simulations are reported and, in general, yields acceptable results.

Acknowledgment

This study is part of a program conducted by GRECO "Grandes Déformations et Endommagement". It was supported through a contract in the case of the 17 - 12 SPH stainless steel (EDF — K0665) and helped by SNECMA in the case of INCO. The authors wish to acknowledge the helpful discussions with Prof. A. Pineau (E.M.P.), Prof. G. Cailletaud (E.M.P.), and J. J. Engel (E.D.F.).

References

1 Trivaudey, F., and Delobelle, P., "High Temperature Creep Damage Under Biaxial Loading, Part I: Experiments," ASME JOURNAL OF ENGINEERING MATERIALS TECHNOLOGY, (1990) to appear.

2 Rabotnov, Y. N., *Creep Problems in Structural Members*, North-Holland, 1969, p. 176-400.

3 Chaboche, J. L., "Continuum Damage Mechanics, Part I: General Concepts; Part II: Damage Growth, Crack Initiation and Crack Growth," ASME *Journal of Applied Mechanics*, Vol. 55, 1988, pp. 59-64, 65-72.

4 Lemaitre, J., "How to Use Damage Mechanics," *Nucl. Eng. and Design*, Vol. 80, 1984, pp. 233-245.

5 Hayhurst, D. R., "Creep Rupture Under Multi-Axial States of Stress," *J. Mech. Phys. Sol.*, Vol. 20, 1972, pp. 381-390.

6 Leckie, F. A., and Hayhurst, D. R., "Constitutive Equations for Creep Rupture," *Acta Met.*, Vol. 25, 1977, pp. 1059-1070.

7 Dyson, B. F., and McLean, D., "Creep of Nimonic 80A in Tension and Torsion," *Met. Sci. J.*, Vol. 2, 1977, pp. 37-45.

8 Cane, B. J., "Creep Cavitation and Rupture in $2^{1/4}$ Cr 1 Mo Steel Under Uniaxial and Multiaxial Stresses," Int. Conf. Mech. Behaviour of Materials, Vol. II, eds. K. J. Miller, R. F. Smith, Pergamon Press, 1979, pp. 173-182.

9 Murakami, S., "Notion of Continuum Damage Mechanics and Its Application to Anisotropic Creep Damage Theory," ASME JOURNAL OF ENGINEERING MATERIALS TECHNOLOGY, Vol. 105, 1983, pp. 99-105.

10 Murakami, S., Sanomura, Y., and Saitoh, K., "Formulation of Cross Hardening in Creep and Its Effect on the Creep Damage Process of Copper," ASME JOURNAL OF ENGINEERING MATERIALS TECHNOLOGY, Vol. 108, 1986, pp. 167-173.

11 Hales, R., "A Method of Creep Damage Summation Based on Accumulated Strain for the Assessment of Creep-Fatigue Endurance," *Fat. of Eng. Mat. and Structure*, Vol. 6, No. 2, 1983, pp. 121-135.

12 Majumdar, S., "Relationship of Creep, Creep-Fatigue, and Cavitation Damage in Type 304 Austenitic Stainless Steel," ASME JOURNAL OF ENGINEERING MATERIALS TECHNOLOGY, Vol. 111, 1989, pp. 123-131.

13 Beziat, J., Diboine, A., Levaillant, C., and Pineau, A., "Creep Damage in a 316 Stainless Steel Under Triaxial Stresses," *IV Int. Sem. on Inelastic Analysis and Life Prediction in High Temperature Environment*, Chicago, Ill., 1983.

14 Levaillant, C., Pineau, A., Yoshida, M., and Piques, R., "Creep Tests on Axisymmetric Notched Bars; Global Displacement Measurements and Metallographic Determination of Local Strain and Damage," *Techniques for Multi-Axial Creep Testing*, Chapter XI, eds. D. J. Gooch and I. M. How, Elsevier Applied Science, 1986, pp. 199-208.

15 Delobelle, P., and Oytana, C., "Etude des Lois de Comportement à Haute Température en "Plasticité-fluage" d'un Acier Inoxydable Austénique," *J. of Nucl. Mat.*, Vol. 139, 1986, pp. 204-227.

16 Delobelle, P., and Oytana, C., "Modeling of 316 Stainless Steel (17 - 12 SPH) Mechanical Properties Using Biaxial Experiments, Part I: Experiments and Basis of the Model; Part II: Model and Simulations," ASME *J. Press. Vessel. Techn.*, Vol.109, 1987, pp. 449-454 and 455-459.

17 Contesti, E., and Cailletaud, G., "Creep-Plasticity Interaction with Coupled Kinematic Hardening. Model and Finite Element Implementation," *Proceedings of Mecamat — Besançon*, France, 1988, pp. I/9, I/34.

18 Murakami, S., and Ohno, N., "A Continuum Theory of Creep and Creep Damage, I.U.T.A.M. Symposium, Leicester, *Creep in Structures*, eds., A. R. S. Ponter and D. R. Hayhurst, Springer-Verlag, 1980, pp. 422-443.

19 Chaboche, J. L., Dang-Van, K., and Cordier, G., "Modelization of the Strain Memory Effect on the Cyclic Hardening of a 316 Stainless Steel," *Proc. of SMIRT 5*, Division L, Berlin, 1979.

20 Ohno, N., "A Constitutive Model of Cyclic Plasticity with a Non-Hardening Strain Region," ASME *Journal of Applied Mechanics*, Vol. 49, 1982, pp. 721-727.

21 Delobelle, P., Thesis, Besançon-France, 1985.

22 Saanouni, K., Thesis, U.T.C. Compiègne, Paris, 1988.